Caractérisation dynamique d'un capteur de flux de chaleur micro-fabriqué

Dynamic characterization of a micro-fabricated heat flux sensor

Himanshi KHARKWAL[1,2*], Eric GAVIGNET[2], Sébastien EUPHRASIE[1], Syed SHAH[2], Abbas HAMIEH[2], Magali BARTHES[1], Lounès TADRIST[3], François LANZETTA[2]

[1]Université Marie et Louis Pasteur, CNRS, institut FEMTO-ST,
F-25000 Besançon, France
[2]Université Marie et Louis Pasteur, CNRS, institut FEMTO-ST,
F-90000 Belfort, France
[3]Université d'Aix-Marseille, CNRS, IUSTI,
Marseille, France
[*](Corresponding author: himanshi.kharkwal@univ-fcomte.fr)

Résumé - L'ébullition, un mécanisme passif permettant d'optimiser le transfert thermique, est essentielle dans de nombreuses applications industrielles. L'objectif de cette étude est de développer un capteur, le "micro-ébulliomètre", capable de mesurer avec précision les températures et les flux thermiques à l'échelle des bulles. Fabriqué à l'aide de techniques de micro-fabrication, il se compose d'une sonde RTD (Détecteur de température à résistance) en platine montée sur une membrane de verre de 40 µm d'épaisseur, d'un micro-réchauffeur intégré à une deuxième sonde RTD en platine et d'un site de nucléation artificiel de 100 µm. Sa caractérisation dynamique dans quatre environnements différents (laser, air chaud, gouttelettes et ébullition en piscine) a révélé des temps de réponse compris entre 40 et 250 ms. La comparaison avec un appareil de mesure de référence de l'ébullition fabriqué par CAPTEC indique que le micro-ébulliomètre offre des performances dynamiques améliorées, ce qui justifie son utilisation pour des études détaillées des phénomènes de transfert de chaleur, en particulier l'ébullition en vase.

Abstract - Boiling, a passive mechanism for optimizing heat transfer, is crucial for many industrial applications. The aim of this study is to develop a sensor, the "micro-boiling meter," capable of accurately measuring temperatures and heat fluxes at the bubble scale. Manufactured using microfabrication techniques, the device incorporates a platinum RTD (Resistance Temperature Detector) probe built on a 40 µm-thick glass membrane, a microheater integrated with a second platinum RTD probe, and a 100 µm artificial nucleation site. Its dynamic characterization in four different environments (laser, hot air, droplet, and pool boiling) revealed response times between 40 and 250 ms. Comparison with a reference boiling meter manufactured by CAPTEC indicates that the microfabricated boiling meter offers improved dynamic performance, supporting its use for detailed studies of heat-transfer phenomena, particularly pool boiling.

Nomenclature

f	frequency, (Hz)
t	time, (s)
Abbreviations	
t_{rise}	characteristic rise time, (ms)
t_{fall}	characteristic fall time, (ms)
R-top	RTD at sensing side
R-bot	RTD at bottom

1. Introduction

Boiling plays a central role in many high-performance thermal systems due to its heat transfer capability, including in energy conversion and electronics cooling. However, despite long-standing research efforts, boiling phenomena remain challenging to predict due to their sensitivity to local conditions. Studying the initial stages of boiling, such as the initiation of nucleate boiling at an isolated site, is a promising way to improve our understanding of the process. Such investigations require measurement techniques that can resolve rapid, highly localized variations in temperature and heat flux.

A wide range of approaches has been developed to quantify heat transfer [1]. High-speed optical diagnostics, including interferometric techniques, enable the detailed visualization of rapid, highly localized thermal processes. However, their reliance on sophisticated instrumentation and clear optical access restricts their broader use. More conventional methods, such as calorimetric [2] and acoustic techniques, have traditionally been used for averaged or steady-state measurements due to their limited transient response. However, recent efforts incorporating data-driven and machine learning frameworks suggest improved performance at higher frequencies [3]. By contrast, inverse heat transfer methods can capture moderate temporal dynamics, though their performance often deteriorate in the presence of measurement noise and fast transients [4].

Boiling heat-transfer measurements can be categorized generally into four groups. Infrared thermography provides non-intrusive, full-field temperature mapping and captures localized boiling features. However, its accuracy depends strongly on surface properties [5]. Subsurface temperature sensing uses embedded sensors to infer heat flux via Fourier's law [6]. While this method is simple and direct, it is limited by pointwise measurements and thermal lag from the substrate. Integrated microheater–sensor arrays enable localized heating and sensing with improved spatial precision [7]; however, their resolution and applicability are constrained by fabrication geometry and complexity. Direct heat flux sensors offer a straightforward voltage-based output and have been used in transient boiling studies [8]. However, their spatial and temporal resolution are ultimately restricted by the internal structure of the sensor and the thermal resistance induced by integration.

Despite significant progress in boiling research, no existing technique combines sub-millimeter spatial resolution, with small temporal response, and minimal disturbance at individual nucleation sites. To address this gap, the present work—carried out within the ANR TraThI (Thermal Transfers at Interfaces) project—develops a novel microfabricated heat flux sensor, the “micro-boiling meter” (µ-BM), capable of generating bubbles at controlled locations while simultaneously measuring local temperature and heat flux. The term “micro” refers to its functional films and membrane, which are microfabricated with micron-scale thicknesses and dimensions. The µ-BM was characterized dynamically under four thermal conditions: laser heating, convective heating, droplet deposition and single-site pool boiling. For droplet deposition test, the µ-BM was also evaluated against a reference boiling meter (BM-2) designed by IUSTI and manufactured by CAPTEC, which incorporates commercial thermopile sensors. The micro-boiling meter demonstrated rapid response times (40–250 ms), high sensitivity and reliable operation across all tested conditions. This ensures sufficient sensitivity and time response for detailed studies of boiling physics and other small-scale thermal phenomena that are beyond the capabilities of conventional sensors.

2. Micro-boiling meter: Design and dimensions

For single bubble pool boiling studies, the device must meet two key requirements: (1) generate a single, controlled bubble, and (2) provide sufficient sensitivity and temporal resolution to capture fluctuations in wall temperature and heat flux. To achieve this, a normal gradient heat flux sensor with an inbuilt nucleation site and heater was selected. The final design (Fig. 1a) was guided by one-dimensional thermal calculations, mechanical evaluations and numerical simulations. The membrane-based structure was selected to reduce thermal inertia related to the substrate.

The fully fabricated view of µ-BM is shown in Fig. 1b. The device integrates a normal gradient heat flux sensor (N-HFS, Fig. 1b), composed of platinum RTDs (Fig. 1c and 1e), a thin-film heater (Fig. 1e), and a 100 µm diameter cylindrical nucleation site (Fig. 1a, 1c and 1d). Unlike conventional designs, the RTDs are directly exposed to the fluid, enabling high-resolution temperature measurement. The heat flux is derived from the temperature gradient across a three-layer substrate (Borofloat 33 membrane, an insulated silicon wafer with a central air cavity, and a thermally oxidized silicon wafer). Two spiral Pt-RTDs monitor temperature: RTD-top (on the membrane, Fig. 1c) and RTD-bot (on the lower wafer, Fig. 1e). The thin films (Ti/Pt, 190–260 nm thick) were optimized for sensitivity and minimal self-heating.

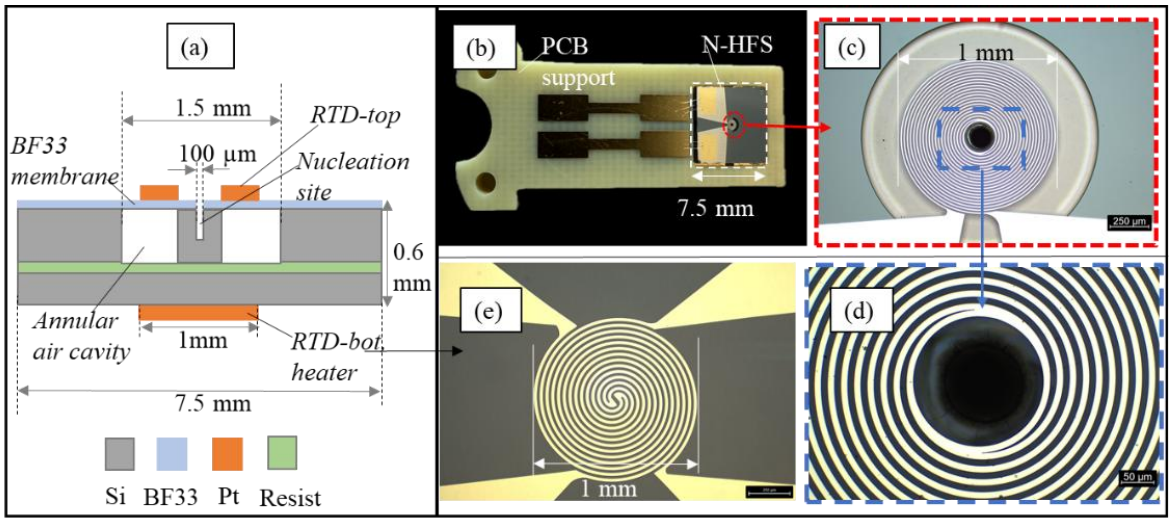

Figure 1: *(a) Schematic of the normal gradient heat flux sensor (N-HFS). (b) The micro-boiling meter showing the N-HFS and highlighting the top sensitive Pt RTD deposited on the Borofloat 33 membrane. (c) Full view of the top Pt-RTD on the Borofloat 33 membrane, showing the central nucleation site. (d) Zoomed view of the nucleation site. (e) Two concentric Pt spirals, one serving as the bottom Pt-RTD and the other as the integrated Pt heater*

3. Experimental setup for dynamic characterization of µ-BM

To assess the dynamic performance of the µ-BM, controlled experiments were carried out under radiative, convective, and droplet deposition conditions. In the drop test, the µ-BM was directly compared with a reference CAPTEC-based boiling meter (BM-2). Finally, its dynamic behaviour was evaluated under pool boiling at different surface inclinations (180° to 90°). For brevity, only two representative orientations are presented here: 150° (near downward-facing) and 0° (upward-facing reference). These orientations effectively capture the influence of inclination on bubble frequency and demonstrate the microfabricated boiling meter's ability to detect nucleate boiling events.

3.1. Experimental setup: Radiative test

The radiative setup, as shown in Fig. 2a, comprises a 200 mW laser source, a mechanical shutter, an attenuator, and a mirror to direct the laser beam onto the surface of the µ-BM. The laser spot diameter was theoretically calculated as 7 mm, and was selected to ensure uniform heating of the sensing area. The top Pt RTD, located on the sensing side, was connected through a Wheatstone bridge and an amplifier to an oscilloscope, to record high-speed temperature and heat flux transients during radiative heating.

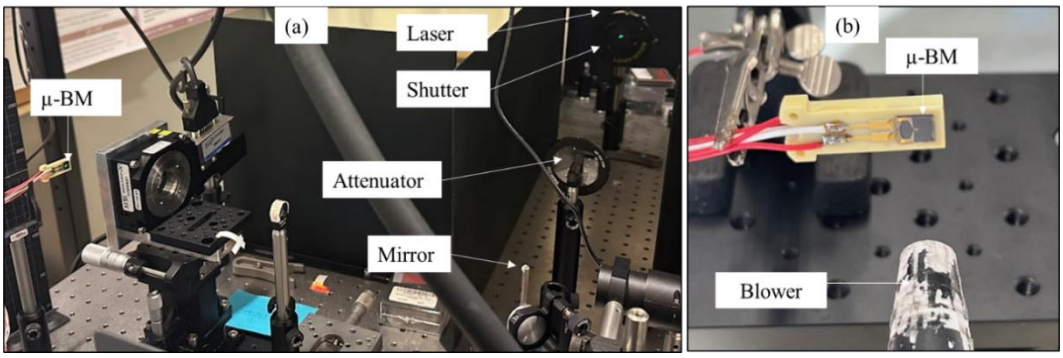

Figure 2*: Experimental setups showing main components for (a) radiative and (b) convective tests*

3.2. Experimental setup: Convective test

The convective setup included a blower supplying hot air (Fig. 2b), a shutter to block airflow until the desired temperature was reached, and the µ-BM positioned in front of the airflow. The top Pt-RTD of the µ-BM was incorporated into a voltage divider circuit with a 10^4 Ω reference resistor. A regulated DC supply provided the excitation voltage, and the output at the divider midpoint was recorded using a National Instruments (NI) data acquisition system.

3.3. Experimental setup: Drop test

In the drop test, a droplet of ultrapure water was deposited onto the sensor surface to assess dynamic response. For comparison with a commercial sensor–based boiling meter, BM-2 equipped with two CAPTEC thermopile sensors (HFS-A and HFS-B) and embedded T-type thermocouples was also evaluated. The BM-2 incorporates 800 µm-thick copper pellets and a 2.5 mm resin insulation layer to limit transverse heat losses. More details on BM-2 can be found in Tadrist *et al.* [8]. Both boiling meters were mounted horizontally on a rigid support and interfaced with National Instruments data acquisition systems. Electrical resistance of the three RTDs of the µ-BM (R-top, R-bot, and R-heater) was measured using an NI 9226 module, while voltage signals from the heat flux sensors and thermocouples of BM-2 were acquired using an NI 9212 module. Data acquisition and system control were implemented in LabVIEW. Ultrapure water was heated to the desired temperature, monitored using a K-type thermocouple, transferred to a pipette, and sequentially deposited onto the BM-2 and the µ-BM. To ensure repeatability, the droplet size, release height, temperature, and deposition procedure were kept identical. A schematic of the experimental setup is shown in Fig. 3a.

3.4. Experimental setup: Pool boiling

The pool boiling experiments were conducted in a cubic stainless-steel test cell with transparent glass windows for optical access (Fig. 3b). The cell was filled with Flutec PP1. Liquid temperature was controlled using four PID-regulated cartridge heaters, while K-type

thermocouples monitored the liquid temperature. System pressure was stabilized using an expansion vessel mounted above the cell. The µ-BM was mounted on a rotatable shaft, enabling surface inclination studies with ±1° accuracy. Its integrated heater was powered by an external supply, with voltage and current monitored using multimeters. For data acquisition, RTD-top and RTD-bot were connected to a NI data acquisition system interfaced with LabVIEW.

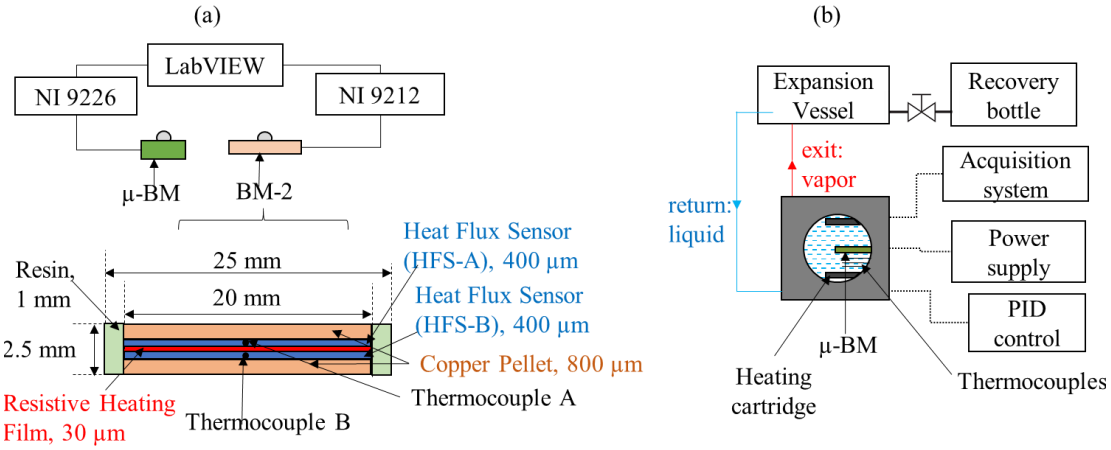

Figure 3: *Schematic of the experimental setups: (a) drop test, showing BM-2 details at the bottom, and (b) pool boiling setup.*

Nucleate boiling was initiated using the integrated platinum heater of the µ-BM, with Joule heating power varied between 0.5 and 0.6 W to control bubble generation. To promote reliable nucleation at the artificial site, the boiling surface was initially oriented downward (180°), after which the orientation was adjusted as required. During experiments, resistance signals from the top and bottom Pt-RTDs were continuously recorded. Bubble dynamics were simultaneously captured with a high-speed camera to correlate boiling events with sensor response. Owing to the linear resistance–temperature relationship of Pt-RTDs, resistance variations directly reflect local temperature fluctuations; therefore, the analysis focuses on temporal signal evolution rather than absolute temperature values.

4. Results and discussion

To evaluate the dynamic response of the µ-BM, a series of controlled experiments were conducted under radiative, convective, and droplet deposition conditions. These tests imposed well-defined thermal transients to assess the sensor's temporal performance under different heat transfer mechanisms. The temporal response was quantified using two characteristic times: the rise time, t_{rise}, defined as the time for the signal to increase from 10% to 90% of its total change and associated with heating from the energy source (laser, hot air, or liquid contact); and the fall time, t_{fall}, defined as the time for the signal to decrease from 90% to 10%, corresponding to natural cooling. For the drop test, the µ-BM was directly compared with BM-2. Finally, the dynamic behaviour of the µ-BM was investigated under pool boiling conditions at two surface orientations (150° and 0°) to evaluate its response during nucleate boiling events.

For the radiative test, the laser was operated at a power of 200 mW with a beam diameter of 7 mm. Exposure was regulated using a mechanical shutter and stopped upon reaching the signal peak. The result is shown in Fig. 4a, the primary y-axis corresponds to the resistance of RTD at sensing side (R-top), the secondary y-axis shows the percentage of response reached, and the x-axis represents time (t). The observed rise and fall times were 250 ms and 280 ms,

respectively. For the second test, under hot-air convection, the µ-BM exhibited a rapid rise time (t_{rise}=202 ms) but a much longer fall time (t_{fall}=1810 ms) (see Fig. 4b and 4c). The quick rise demonstrates that the µ-BM responds effectively to the onset of convective heating, thanks to its low thermal mass and surface-localized sensing elements. The longer cooling time is dominated by environmental and structural thermal inertia, which can include slower heat removal via natural convection, heat retention by the surrounding air and sensor mount, and the thermal mass of the substrate and sensor body.

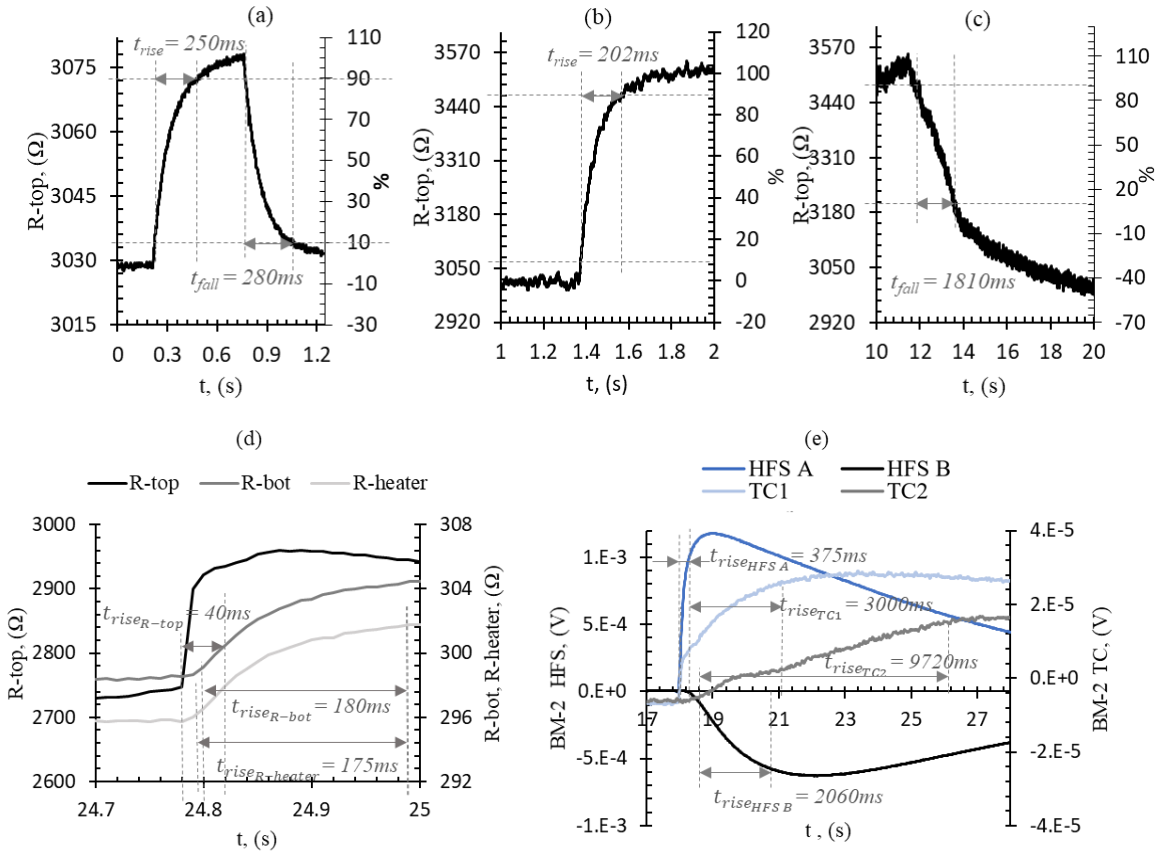

Figure 4: *Dynamic response of the boiling meters under different thermal excitations: (a) radiative heating using laser irradiation, (b) convective heating phase under hot-air flow and (c) subsequent convective cooling phase after airflow interruption, (d) drop test response of the µ-BM showing rapid temperature transients due to direct liquid–surface contact, (e) drop test response of the reference boiling meter (BM-2), illustrating its comparatively slower dynamic behaviour*

Figure 4d presents the µ-BM response during droplet deposition at 73.6 °C. It represents, the different resistances: sensing RTD, R-top on the primary y-axis, and RTD on bottom R-bot and Pt heater R-heater on the secondary y-axis, and time along the x-axis. The results show, all three resistive elements responded, with rise times of approximately 40 ms for R-top, 180 ms for R-bot, and 175 ms for R-heater. For BM-2, the graph displays the HFS voltages on the primary y-axis, thermocouple voltages on the secondary y-axis, and time on the x-axis. A pronounced voltage drop is observed in HFS A (face with drop), with a rise time of ~375 ms. A delayed response is seen in HFS B, which is on the opposite face of the drop, with a rise time of ~2060 ms, while the embedded thermocouples responded over several seconds due to higher thermal mass and internal placement.

Figure 5a and 5b shows the results of µ-BM from pool boiling experiments. The black curve shows R-top, which is the resistance of the RTD in direct contact with bubbles nucleating at the

artificial site, and the grey curve shows R-bot, which is on the opposite side. Two surface orientations 150° and 0° were tested, with an uncertainty of ±1°. For both angles, the R-top exhibits clear oscillations corresponding to individual bubble nucleation and departure, with measured bubble frequencies of ~8.5 Hz and ~24 Hz for 150° and 0°, respectively, while the bottom RTD remains relatively constant.

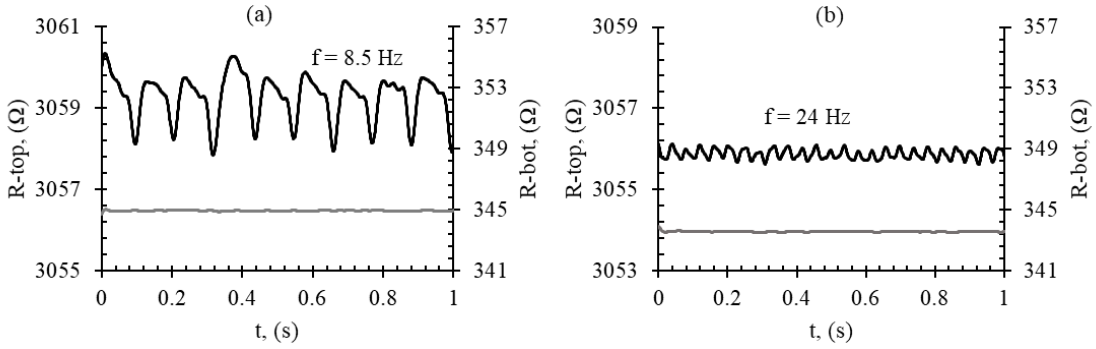

Figure 5: *µ-BM response during pool boiling: R-top and R-bot at surface orientations (a) 150° and (b) 0°, showing oscillations associated with individual bubble nucleation and departure events*

Table 1 summarizes the characteristic parameters obtained under the different test conditions. The dynamic characterization of the µ-BM demonstrates its ability to capture rapid thermal transients under radiative, convective, and droplet deposition conditions. The differences in rise times are directly related to the heat transfer mechanism and the amount of energy effectively delivered to the sensor. In the drop test, the liquid droplet is in direct contact with the RTD, resulting in a very high local heat flux and the fastest t_{rise} of ~40 ms for the R-top. Convective heating involves hot air at an elevated temperature transferring energy through forced convection, resulting in a moderate t_{rise} of ~202 ms. Radiative heating uses a 200 mW laser to spread energy over a 7 mm spot, producing a slightly longer t_{rise} of ~250 ms. Fall times are primarily governed by thermal inertia, including that of the substrate, sensor structure, and surrounding environment. Overall, these results demonstrate that the µ-BM can reliably detect rapid, localised temperature fluctuations and bubble dynamics across a range of heating conditions, thus validating its suitability for detailed studies of boiling and small-scale heat transfer phenomena.

Test	Boiling meter	Parameter studied	Value
Radiative	µ-BM	t_{rise} for R-top (ms)	250
	µ-BM	t_{fall} for R-top (ms)	280
Convective	µ-BM	t_{rise} for R-top (ms)	202
	µ-BM	t_{fall} for R-top (ms)	1810
Droplet	µ-BM	t_{rise} for R-top (ms)	40
	µ-BM	t_{rise} for R-bot (ms)	180
	µ-BM	t_{rise} for R-heater (ms)	175
	BM-2	t_{rise} for HFS A (ms)	375
	BM-2	t_{rise} for HFS B (ms)	2060
	BM-2	t_{rise} for TC A (ms)	3000
	BM-2	t_{rise} for TC B (ms)	9720
Pool boiling	µ-BM	f at 150° surface inclination (Hz)	8.5
	µ-BM	f at 0° surface inclination (Hz)	24

Table 1: Summary of characteristic parameters obtained in different tests

5. Conclusion

The “micro-boiling meter” (µ-BM), a microfabricated heat flux sensor, was developed to measure temperatures and heat fluxes at the bubble scale. It integrates a platinum RTD probe built on a 40 µm-thick glass membrane, a microheater integrated with another platinum RTD probe and a 100 µm nucleation site. The µ-BM was characterised dynamically under radiative, convective, droplet and pool boiling conditions. Rise times ranged from ~40 ms for drop test to 250 ms under laser irradiation, with convective heating showing an intermediate rise time (202 ms), reflecting the influence of the heat transfer mechanism and energy flux. In pool boiling experiments, the µ-BM successfully captured individual bubble nucleation and departure, with measured bubble frequencies of ~8.5 Hz and ~24 Hz at surface orientations 150° and 0°, respectively. In the drop test, the µ-BM was compared with a reference boiling meter (BM-2) and demonstrated enhanced dynamic performance. The results indicate that the µ-BM effectively captures fast, localized thermal events, providing a reliable platform for detailed studies of boiling and microscale heat transfer.

References

[1] T. E. Diller and M. Kutz, “Heat flux measurement,” *Mechanical Engineers’ Handbook, Volume 4: Energy and Power*, vol. 4, p. 285, 2015.

[2] K. Dejima, O. Nakabeppu, Y. Nakamura, T. Tsuchiya, and K. Nagasaka, “Three-point MEMS heat flux sensor for turbulent heat transfer measurement in internal combustion engines,” *International Journal of Engine Research*, vol. 20, no. 7, pp. 696–705, Sep. 2019, doi: 10.1177/1468087418770308.

[3] C. Dunlap, H. Pandey, E. Weems, and H. Hu, “Nonintrusive heat flux quantification using acoustic emissions during pool boiling,” *Appl Therm Eng*, vol. 228, p. 120558, Jun. 2023, doi: 10.1016/J.APPLTHERMALENG.2023.120558.

[4] M. Hafid and M. Lacroix, “Inverse method for simultaneously estimating multi-parameters of heat flux and of temperature-dependent thermal conductivities inside melting furnaces,” *Appl Therm Eng*, vol. 141, pp. 981–989, Aug. 2018, doi: 10.1016/J.APPLTHERMALENG.2018.06.041.

[5] M. Može, A. Hadžić, M. Zupančič, and I. Golobič, “Boiling heat transfer enhancement on titanium through nucleation-promoting morphology and tailored wettability,” *Int J Heat Mass Transf*, vol. 195, Oct. 2022, doi: 10.1016/j.ijheatmasstransfer.2022.123161.

[6] R. Jaswal, A. Sathyabhama, K. Singh, and A. V. V. R. P. Yandapalli, “Experimental and numerical investigation of pool boiling heat transfer from finned surfaces,” *Appl Therm Eng*, vol. 233, p. 121167, Oct. 2023, doi: 10.1016/J.APPLTHERMALENG.2023.121167.

[7] C. Hutter, K. Sefiane, T. G. Karayiannis, A. J. Walton, R. A. Nelson, and D. B. R. Kenning, “Nucleation site interaction between artificial cavities during nucleate pool boiling on silicon with integrated micro-heater and temperature micro-sensors,” *Int J Heat Mass Transf*, vol. 55, no. 11–12, pp. 2769–2778, May 2012, doi: 10.1016/j.ijheatmasstransfer.2012.02.014.

[8] L. Tadrist, H. Combeau, M. Zamoum, and M. Kessal, “Experimental study of heat transfer at the transition regime between the natural convection and nucleate boiling: Influence of the heated wall tilt angle on the onset of nucleate boiling (ONB) and natural convection (ONC),” *Int J Heat Mass Transf*, vol. 151, p. 119388, Apr. 2020, doi: 10.1016/J.IJHEATMASSTRANSFER.2020.119388.

Acknowledgements

The authors thank the French National Research Agency (ANR) for its financial support of the TraThI project (ANR-21-CE50-0009-01 grant). This work was carried out within the framework of the EIPHI graduate school (ANR-17-EURE-0002 grant). This work was supported by the French RENATECH network and its FEMTO-ST technology center.